SUBDUCTION INITIATION BY STAGNANT LID CONVECTION IN SPHERICAL SHELL GEOMETRY: IMPLICATIONS FOR MARS. C.C. Reese and V.S. Solomatov, *Department of Earth and Planetary Sciences, Washington University, St. Louis, MO 63130*.

Introduction. Rheological constraints suggest that for viscous creep alone, Martian mantle convection occurs in the stagnant lid regime where the lithosphere is immobilized due to high viscosity. On the other hand, the possibility of lithospheric recycling early in Mars history has been discussed in the context of surface morphology (Sleep, 1994), magnetic anomalies (Connerney et al., 1999) and magnetic field generation (Nimmo and Stevenson, 2000). Subduction occurs only if brittle fracture sufficiently weakens the upper lithosphere. Initiation of subduction in the stagnant lid regime may play a key role in transient lithospheric mobilization during Mars early evolution.

Numerical simulations of time dependent, stagnant lid convection in an internally heated spherical shell are performed in order to obtain scaling relationships for convection induced lid stresses. As was found in two-dimensional simulations, stagnant lid convection in spherical shell geometry requires a very weak lithosphere (Solomatov, 2004a;b) for initiation of subduction.

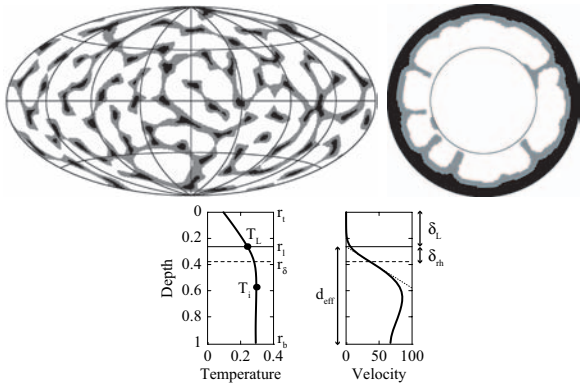

Figure 1: Thermal structure of internally heated, time-dependent stagnant lid convection in a spherical shell (top). The temperature distribution on the spherical surface at the base of the stagnant lid (left). Fluid colder than the spherically averaged temperature is indicated by gray and black. The temperature distribution on an equatorial cross section (right). Instability involves only a small fraction (gray) of the cold thermal boundary layer. The coldest part (black) is stagnant and does not participate in convection. Spherically averaged temperature and velocity in the shell (bottom). The bottom of the lid (solid horizontal line) is defined as the intersection of the maximum velocity gradient (dotted line on the velocity graph) with the depth axis. The bottom of the cold boundary layer is indicated with a dashed horizontal line. The rheological sublayer is bounded by the horizontal solid and dashed lines. The interior temperature is indicated by the circle.

Numerical simulations. The finite element code TERRA (Baumgardner, 1985; Bunge and Baumgardner, 1994) was utilized to perform numerical simulations of stagnant lid convection in a spherical shell. The boundary conditions are free slip, the shell is internally heated, and the bottom boundary is thermally insulated. An exponential viscosity law was considered (differences between an exponential and Arrhenius law near the lid surface are unimportant for the analyses presented here). Linear stability analysis (Stengel et al., 1982) suggests that the transition to stagnant lid convection occurs for a viscosity contrast across the cold boundary layer of $\approx 3 \times 10^3$. All simulations considered in the study were in the asymptotic large viscosity contrast regime (Figure 2) and each case is run until the solution adjusts to initial conditions, an equilibrium between internal heat production and heat loss is reached, and a time dependent state is established with global quantities fluctuating about a mean value.

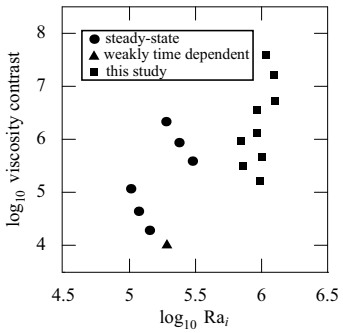

Figure 2: Parameter range explored in this and previous works is shown in interior Rayleigh number – viscosity contrast space.

Scaling relationships. A Nusselt number is defined in terms of the total energy production in the shell (Reese et al., 1999),

$$Nu = \frac{F\,d}{k(T_i - T_s)} = \frac{\rho\,H\,d\,r_t\,(1 - r_b^3/r_t^3)}{3k(T_i - T_s)} \ . \qquad (1)$$

where F is the surface heat flux, d is the shell thickness, k is the thermal conductivity, T_i is defined as the maximum interior temperature (Figure 1), T_s is the surface temperature, ρ is the density, H is the radiogenic heating rate, r_t is the outer radius, and r_b is the inner radius.

Scaling theory and boundary layer stability analysis (Solomatov, 1995) suggest that the interior shear stress generated by sinking plumes should scale as

$$\tau_i \sim \rho\alpha g \Delta T_{rh} \delta_{rh} \ , \qquad (2)$$

where α is the coefficient of thermal expansion, g is the acceleration due to gravity, ΔT_{rh} is the driving temperature difference across the rheological sublayer (Figure 1) and δ_{rh} is the

rheological sublayer thickness. The interior stress is defined as the spherically averaged second invariant of the deviatoric stress tensor at 3/4 of the total shell depth (Figure 3).

Lid stresses can be generated by the lid base slope (Fowler, 1985) as well as sinking plumes (Solomatov, 2004a). The lid stress τ_{lid} is estimated by extrapolating the stress profile beneath the stress boundary layer to the surface (Figure 3). Lid stresses generated by sinking plumes should scale like τ_i. The alternative large lid slope scaling is not addressed here.

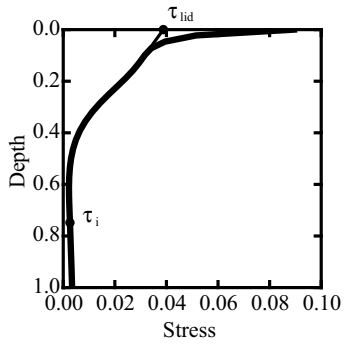

Figure 3: Stress (second invariant of the deviatoric stress tensor normalized by $\eta_s \kappa / d^2$) distribution for the case corresponding to Figure 1.

Based on the numerical results, the scaling relationships obtained for the exponential viscosity law can be applied to temperature and pressure dependent Arrhenius viscosity law (Karato and Wu, 1993),

$$\eta = \frac{\mu}{2A} \left(\frac{h}{B}\right)^m \exp\left(\frac{Q}{RT}\right) = b \exp\left(\frac{Q}{RT}\right) , \quad (3)$$

where μ is the shear modulus, A is the preexponential factor, h is the grain size, B is the Burgers vector, $Q = E + pV$ is the activation enthalpy, E is the activation energy, p is the hydrostatic pressure, V is the activation volume, R is the gas constant, T is the temperature and $b = \mu/(2A)\,(h/B)^m$ is a constant. With the following definitions of the Frank-Kamenetskii parameter θ and interior Rayleigh number Ra_i (Reese et al., 1999; Solomatov and Moresi, 2000),

$$\theta = \frac{\Delta T E}{R T_i^2} - \frac{p_i V T_s}{R T_i^2} , \quad (4)$$

$$Ra_i = \frac{\rho \alpha g \Delta T d^3}{\kappa b \exp\left[(E + p_i V)/(R T_i)\right]} , \quad (5)$$

where p_i is the pressure at the bottom of the thermal boundary layer and $\Delta T = T_i - T_s$, the heat flux

$$F = k \frac{\Delta T}{d} Nu , \quad (6)$$

where

$$Nu = 0.67\, \theta^{-4/3}\, Ra_i^{1/3} . \quad (7)$$

The interior stress

$$\tau_i = 0.1\, \rho \alpha g\, \theta^{-2}\, \frac{k}{F} , \quad (8)$$

and lid stress

$$\tau_{lid} = 2.2\, \rho \alpha g\, \theta^{-2}\, \frac{k}{F} . \quad (9)$$

Results. Figure 4 shows results for Mars. The scaling laws for the interior and lid stresses are similar to those obtained in two dimensions by Solomatov (2004a;b). Since lid stress is the major factor in subduction initiation, it is expected that the critical yield stress for subduction initiation by stagnant lid convection in three dimensions should be similar to that obtained in two-dimensional studies, ~ 1 MPa for Mars (Solomatov, 2004a;b). A direct simulation of subduction initiation in three dimensional spherical shell geometry is being developed to test this prediction.

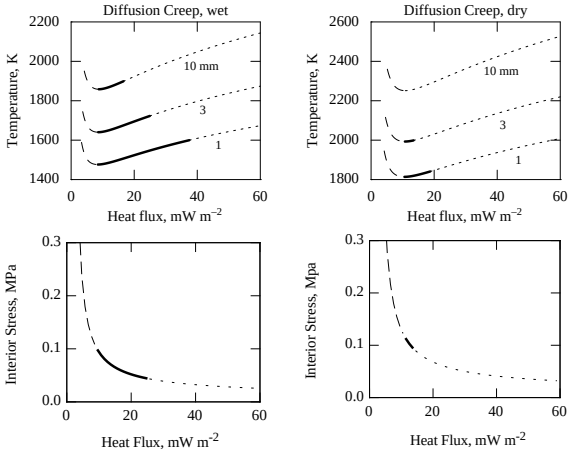

Figure 4: (top) Martian mantle temperature in the stagnant lid regime for diffusion creep of wet and dry olivine labeled by grain size. For a given temperature, there are stable (solid line) and unstable (dashed line) solutions as a consequence of pressure dependent viscosity (Reese et al., 1999; Solomatov and Moresi, 2000). Dotted line indicates a partially molten mantle. (bottom) The interior viscous stress is not affected much by grain size variations and is shown for h = 3 mm.

References.

Baumgardner, J. Stat. Phys., *39*, 501, 1985
Bunge and Baumgardner, Comput. Phys., *9*, 201, 1994
Connerney et al., Science, *284*, 794, 1999
Fowler, Stud. Appl. Math., *72*, 1, 1985
Karato and Wu, Science, *260*, 771, 1993
Nimmo and Stevenson, J. Geophys. Res, *105*, 11969, 2000
Reese et al., Icarus, *139*, 67, 1999
Sleep, J. Geophys. Res., *99*, 5639, 1994
Solomatov, Phys. Fluids, *7*, 266, 1995
Solomatov, J. Geophys. Res., *109*, 10.1029/2003JB002628, 2004a
Solomatov, J. Geophys. Res., *109*, 10.1029/2004JB003143, 2004b
Solomatov and Moresi, J. Geophys. Res., *105*, 21795, 2000
Stengel et al., J. Fluid Mech., *120*, 411, 1982